LA-UR -90-413

Los Alamos National Laboratory is operated by the University of California for the United States Department of Energy under contract W-7405-ENG-36.

LA-UR--90-413

DE90 007622

TITLE *Harmonic Generation Mechanisms in Short-Wavelength Free-Electron Lasers*

AUTHOR(S) *Mark J. Schmitt*

SUBMITTED TO *Proceedings of the Free Electron lasers and Applications Conference held as part of the OE/LASE symposium*
Los Angeles, CA
January 15 19, 1990

DISCLAIMER

Los Alamos Los Alamos National Laboratory
Los Alamos, New Mexico 87545

Harmonic generation mechanisms in short-wavelength free-electron lasers

Mark J. Schmitt

Los Alamos National Laboratory, P. O. Box 1663
MS E531, Los Alamos, New Mexico 87545

ABSTRACT

The physical mechanisms that contribute to harmonic radiation in free-electron laser systems are examined. Mathematical models for the spontaneous and coherent-spontaneous emission in plane-polarized wigglers are given. How these models are used to perform numerical simulations is discussed. Modifications of the models to incorporate non-ideal free-electron laser effects are reviewed.

1. INTRODUCTION

The radiation from relativistic electrons in free electron lasers (FELs) is concentrated in narrow frequency bands centered at integer multiples of the resonant frequency. The narrow bandwidth of this radiation is caused by interference of the radiation from each of the N periods of the wiggler. The electromagnetic radiation produced at twice the resonant frequency (second harmonic) is a consequence of the finite transverse dimensions of the electron beam [1,2]. Radiation at harmonic frequencies above the second harmonic appears as a result of doubly-periodic oscillations in the electron's velocity inside the wiggler[3]. The power observed at the harmonic frequencies can vary significantly depending on the strength of the wiggler magnetic vector potential[4]. Additional coupling to the harmonic frequencies can also occur when the electron, optical and wiggler axes are misaligned[5]. To some degree, such misalignment will exist in any physical system in the form of electron beam offsets, wandering of the electron beam inside the wiggler due to field errors and betatron motion of the single-electron trajectories.

An electron beam passing through a wiggler will radiate spontaneously due to the random distribution of its individual electron constituents. The characteristics of this incoherent radiation can be analytically determined[5]. Alternatively, if the wiggler is long enough or some type of optical feedback is provided, the spontaneous radiation can grow into a large coherent signal as the electrons in the beam begin to bunch[6]. The extent of the bunching is critically dependent on the radiation wavelength (since bunching must occur at this wavelength) and the statistical characteristics of the electron beam. Proper analysis of such a system can be accomplished through numerical simulation[7,8]. By incorporating the inhomogeneity of the electron radiators, i.e., the unique three-dimensional position, velocity and field vectors experienced by each electron, an accurate prediction of the fundamental and harmonic radiation output can be made.

In the quest for coherent short-wavelength radiation one is interested in determining the level of the harmonic coherent-spontaneous emission in FELs. Plane-polarized wigglers lend themselves to harmonic production owing to the non-uniform axial component of the electrons' motion in the sinusoidal wiggler magnetic field. Therefore, the following discussions will assume a plane-polarized wiggler field configuration. To model as many effects as possible one should begin with the most general description of the electron radiation source. Short of modeling the exact wiggle trajectory of each electron[9], a distributed transverse source function for each electron can be used[10]. This theory is valid assuming one confines the analysis to the framework of a single-frequency coherent-spontaneous emission model. By definition the distributed model assumes the electromagnetic source for each electron is *distributed* over its wiggle amplitude. Using this model, harmonic coupling caused by misalignments and transverse gradients is automatically included. In the limiting case where the guiding centers of the electrons travel parallel to the wiggler axis, the distributed source model predicts the generation of even harmonic radiation with odd-symmetry in the electron wiggle

plane and odd harmonic radiation patterns with even transverse symmetry.

In Section 2. a brief review of the theory of spontaneous emission for typical FEL configurations is given. The rest of the paper is devoted to the understanding and modeling of the various effects that contribute to coherent-spontaneous harmonic emission in FELs. In Section 3. a description of the theory for harmonic radiation from plane-polarized wiggler magnetic fields caused by non-uniform axial electron motion, electron density gradients, transverse electron drift motion, transverse wiggler magnetic field gradients and harmonic Fourier components of the wiggler magnetic field is given. The conclusions, including one person's view of what lies ahead in the area of FEL harmonic theory and simulation, are contained in Section 4.

2. SPONTANEOUS EMISSION

Wigglers are used as insertion devices in high energy storage rings to boost the power levels of available incoherent electromagnetic radiation. The simplest configuration is a plane-polarized wiggler of length $L_w = N\lambda_w$ and peak magnetic field strength B_w, driven by an electron beam of energy γmc^2. The energy radiated by each electron of charge $q = -e$ per unit solid angle and frequency bandwidth is given by[5]

$$\left.\frac{d^2I_0}{d\Omega d\omega}\right|_f = \frac{16e^2N^2\gamma^2}{c}\left(\frac{\sin\nu_f}{\nu_f}\right)^2\left(\frac{f\xi}{a_w}\right)^2\left[\left(\frac{\gamma\theta}{a_w}\right)^2 A_{0,f}^2 + \frac{\gamma\theta}{a_w}\cos\phi A_{0,f}A_{1,f} + A_{1,f}^2\right] \tag{1}$$

where

$$A_{a,f} = (-1)^{f+a}\sum_{n=-\infty}^{\infty}(-1)^n J_n(f\xi)[J_{f-2n-a}(f\sigma) + J_{f-2n+a}(f\sigma)] \tag{2}$$

$$\nu_f = \pi N\left[f - \frac{\lambda_w}{2\gamma^2\lambda_r}(1 + a_w^2/2 + \gamma^2\theta^2)\right]$$

$$f\sigma = \frac{8(f\xi)(\gamma\theta)}{a_w}\cos\phi \tag{3}$$

$$\xi = \frac{a_w^2}{4(1 + a_w^2/2 + \gamma^2\theta^2)} \tag{4}$$

and

$$a_w = \frac{|e|B_w\lambda_w}{2\pi mc^2} \tag{5}$$

is the normalized wiggler magnetic vector potential. The radiation wavelength is λ_r, f is the harmonic number and $J_m(z)$ represents the Bessel function of the first kind of order m. Here it has been assumed that the wiggler lies along the z-axis and the angles θ and ϕ are formed by the intersection of the line of observation, call it $\hat{n}$, with the z-axis and the angle made by the intersection of the projection of $\hat{n}$ onto the xy-plane with the x-axis, respectively. The harmonic radiation pattern described in Eq.(1) has multiple lobes where the number of lobes is equal to the harmonic number. The majority of the radiation is contained within a forward cone of angle $\theta \simeq 1/\gamma$.

In principle, this radiation can be enhanced by constructing a composite wiggler formed by two wigglers each having N magnetic periods and separated by a distance L_d. The radiation from this configuration is given in terms of Eq.(1) as[11]

$$\left.\frac{d^2I}{d\Omega d\omega}\right|_f = 2\left.\frac{d^2I_0}{d\Omega d\omega}\right|_f\{1 + \cos[2\pi(N + N_d)]\} \tag{6}$$

where N_d is the number of optical wavelengths an electron falls behind the optical wave in the dispersive section between the wigglers. Dispersive sections containing a magnetic field are commonly used to reduce the overall length between the wiggler sections. The maximum enhancement of a factor of 2 in power from this (optical klystron) configuration cannot be achieved unless an electron beam of sufficient quality can be

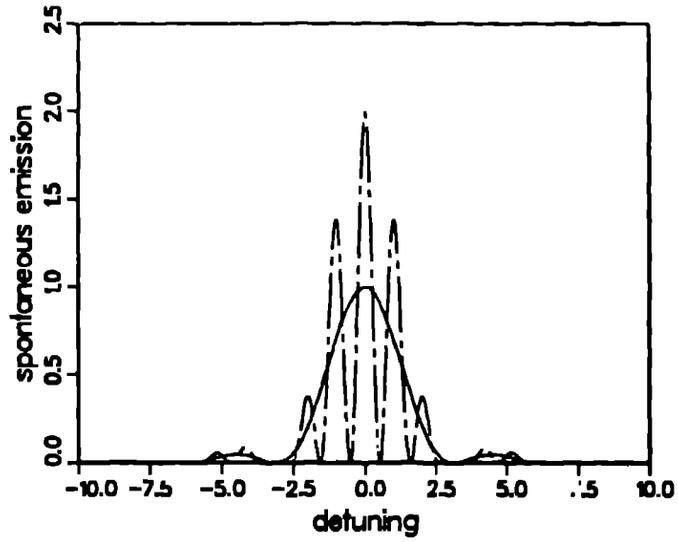

Figure 1. Characteristic lineshapes of the spontaneous emission from a single electron for both the single wiggler (solid line) and the optical klystron (dashed line) configuration. An equal number of wiggler periods was assumed for each configuration.

produced. Examples of the characteristic lineshapes of the spontaneous emission for both the single wiggler and the optical klystron configuration are given in Figure 1.

To achieve harmonic output power above the spontaneous level one must achieve $\epsilon \leq \lambda_r$, where ϵ represents the phase space area ($\pi \times$ emittance) of the electron beam, (in at least some spatial section of the electron beam) so that bunching can occur. For this case the coherent-spontaneous emission must be calculated.

3. COHERENT SPONTANEOUS EMISSION

As previously mentioned, coherent-spontaneous emission arises due to the bunching of the electron beam. In an oscillator or amplifier this bunching is normally produced by the interaction of the electrons with radiation at the fundamental frequency. Since the bunching is a non-linear process, small axial density components are produced at the harmonics of the fundamental bunching wavelength. Coherent harmonic emission can then take place, where the strength of the radiation source is proportional to the amplitude of the density component at the harmonic of interest, and the sum over transverse space of the distributed sources from each electron. The analytical form of the distributed electron sources has been previously derived[10] and only the results of the formalism are of interest here.

The analysis of coherent radiation in FELs typically begins with the wave equation in the paraxial limit. The paraxial approximation is ideally suited for the analysis of the tightly collimated coherent emission from FELs. Within the confines of this approximation, the wave equation for the linearly polarized complex electric field from a plane polarized wiggler has the form[12]

$$\left[2ifk_s\frac{d}{dz}+\frac{\partial^2}{\partial\vec{r}_\perp^2}\right]E_\perp^f=-\frac{i8\pi fk_s}{\lambda_s c}\int_z^{z+\lambda_s}d\zeta J_\perp(x,y,\zeta)e^{-if[k_s(\zeta-z)-\omega_s t]} \qquad (7)$$

where $k_s = 2\pi/\lambda_s = \omega_s/c$ is the fundamental optical wavenumber, c is the speed of light, f is the harmonic number and $J_\perp$ is the transverse current given by

$$J_\perp(x,y,z(t))=-ec\sum_{i=1}^{N_{part}}\frac{a_{wi}}{\gamma_i}\delta(z-z_i(t))\,\delta(x-x_{0i}-\beta_{x0i}z)\delta(y-y_{0i}-\chi_i\sin k_w z-\beta_{y0i}z) \quad . \qquad (8)$$

The sum over i represents the contributions from all the electrons in a ponderomotive wavelength ($\lambda_{pond}^{-1} = \lambda_s^{-1} + \lambda_w^{-1}$). Here we have assumed a plane polarized wiggler magnetic field with period λ_w and amplitude $\vec{B} = \hat{x} B_w \sin k_w z$. The electrons have charge, $q = -e$, and energy, γmc^2, such that they wiggle in the y-direction with their transverse positions given by $y = y_{0i} + \chi_i \sin k_w z + \beta_{y0i} z$ where $\chi_i \simeq \frac{a_w(x_{0i}, y_{0i})}{\gamma_z k_w}$ is the oscillation amplitude of the i^{th} electron and a_w is the wiggler vector potential given in Eq.(5). The quantities (x_{0i}, y_{0i}) and $(\beta_{x0i}, \beta_{y0i})$ are the guiding center position and transverse drift velocities of of the i^{th} electron. To obtain a source function dependent on the electron's transverse y position alone, we average over a wiggler period yielding[10]

$$S_i^o(y) = \frac{i8cfk_s k_w}{\lambda_s} e^{-if\psi_i} \cos\{f[\xi \sin 2\theta_r(y) + \theta_r(y)]\} e^{if\sigma \sin\theta_r(y)} \tag{9}$$

for the odd harmonics and

$$S_i^e(y) = -\frac{8cfk_s k_w}{\lambda_s} e^{-if\psi_i} \sin\{f[\xi \sin 2\theta_r(y) + \theta_r(y)]\} e^{if\sigma \sin\theta_r(y)} \tag{10}$$

for the even harmonics where ξ is the interaction strength parameter given in analogy with Eq.(4) by

$$\xi = \frac{a_w^2}{4(1 + a_w^2/2 + \gamma^2 \beta_{\perp 0i}^2)} \tag{11}$$

and σ is the angular coupling factor defined

$$\sigma = 8\xi \left(\frac{\beta_{y0i}}{a_w/\gamma}\right) \tag{12}$$

Note that the bracketed term in Eq.(12) is a ratio of the transverse drift velocity of an electron to its peak wiggle velocity. This ratio must be small for these results to be valid. Comparing Eq.(12) to Eq.(3) one sees that the observation angle θ in the spontaneous emission expression has been replaced by the electron misalignment angle in the wiggler $\beta_{y0i} \simeq \beta_{y0i}/\beta_z$. The transverse source functions in Eqs.(9) and (10) are a function of $\theta_r(y)$ given by

$$\theta_r(y) = \sin^{-1}\left(\frac{y - y_{0i}}{\chi_i}\right) \qquad y_{0i} - \chi_i \le y \le y_{0i} + \chi_i \tag{13}$$

where we explicitly express the limits of $\theta_r(y)$, confining them to the transverse range of each electron. The source functions are complex quantities except when the electron is perfectly aligned with the wiggler axis ($\sigma \propto \beta_y \Rightarrow 0$). The electron guiding center is at the point $y = y_{0i}$ and the width of the curve reflects the transverse wiggle range of the electron. Plots of the source functions including angular effects with $\sigma = \xi = 1/6$ are given in Figures 2a,b for the fundamental and second harmonic. Since the source functions are complex, the the real and imaginary parts have been plotted with dot-dash and dotted lines, respectively. For reference, the solid line plots the source function for $\sigma = 0$. Note that the real part of the source function is only slightly modified from its $\sigma = 0$ value despite the large value of σ assumed for these calculations. As seen from Figure 2, misalignment of an electron in the wiggler introduces coupling to modes with the opposite transverse symmetry compared to the perfectly aligned case.

To accurately model the radiation pattern of an ensemble of electrons, the distributed transverse source dependence of the individual electrons must be retained. This can be be done by converting the smoothly varying distributed source functions of Eqs.(9) and (10) into discrete (δ-function) sources. For simulation purposes, these discrete sources can then be interpolated onto a numerical gird. The lowest order discrete source for an electron is just a δ-function located at the guiding center position of the electron. The amplitude of this source is given by the transverse average of the distributed source functions. This term is referred to as the monopole source term and is identical to the results obtained from a one-dimensional treatment[5,10].

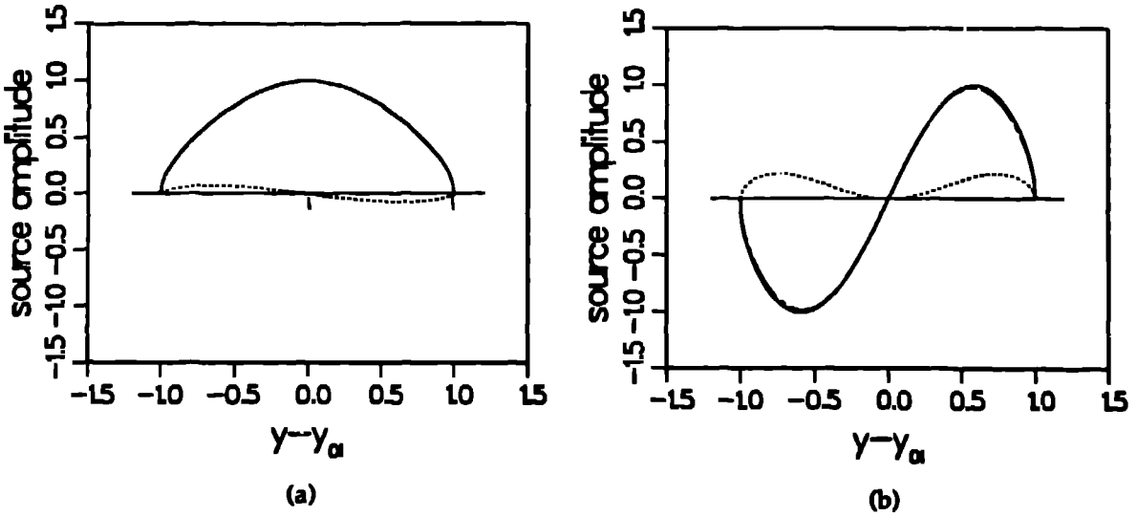

Figure 2. Plots of the distributed source functions including angular effects with $\sigma = \xi = 1/6$ for (a) the fundamental and (b) second harmonic. The real and imaginary parts have been plotted with dot-dash and dotted lines, respectively. For reference, the solid line plots the source function for $\sigma = 0$. Note that the large imaginary part introduces a source with opposite symmetry from the $\sigma = 0$ reference case.

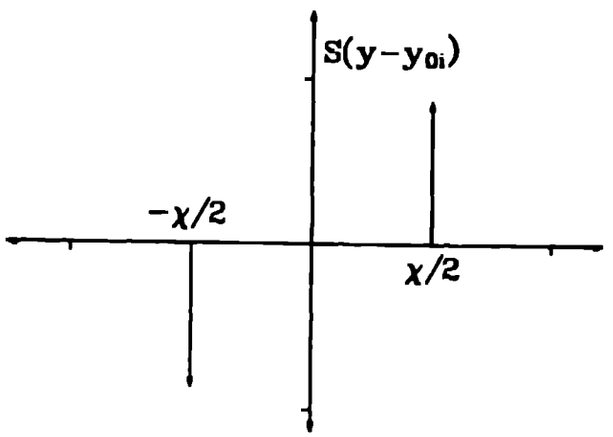

Figure 3. The discrete dipole source function for the second harmonic. The δ-function sources have been positioned half the distance from the guiding center to the wiggle extrema.

As seen from Eq.(10) the lowest order amplitude for the even harmonics in the limit $\sigma \Rightarrow 0$ is zero due to the odd symmetry of the sine term. To obtain a nonvanishing amplitude for the even harmonics in this limit we must go to higher order. The next order discrete source for an electron would be a pair of δ-functions in an odd configuration as shown in Figure 3. This term is referred to as the dipole source term. The amplitudes for this source and the third order discrete source (tripole) have been derived elsewhere[10].

The wave equation including the three discrete source terms can now be written

$$\left[2ijk_s\frac{d}{dz} + \frac{\partial^2}{\partial \tilde{r}_\perp^2}\right] E_\perp^j = \sum_j^{1,2,3} S_j(y) \tag{13}$$

where the three source terms on the right-hand side are given by:

- Mono-pole term

$$S_1(y) = \left\langle \frac{i4\pi I f k_s a_{w,l}}{c} K_f^{(1)}(\xi,\sigma)\delta(y-y_{0i})\frac{e^{-if\psi}}{\gamma} \right\rangle_e \tag{14}$$

- Di-pole term

$$S_2(y) = \left\langle \frac{4\pi I f k_s a_{w,l}}{c} K_f^{(2)}(\xi,\sigma)\frac{1}{2}[\delta(y-y_{0i}-\chi/2)-\delta(y-y_{0i}+\chi/2)]\frac{e^{-if\psi}}{\gamma} \right\rangle_e \tag{15}$$

- Tri-pole term

$$\begin{aligned} S_3(y) = -\Bigg\langle & \frac{i4\pi I f k_s a_{w,l}}{c}[K_f^{(1)}(\xi,\sigma) - K_f^{(3)}(\xi,\sigma)] \\ & \times \left\{\delta(y-y_{0i}) - \frac{1}{2}[\delta(y-y_{0i}-\chi/2)+\delta(y-y_{0i}+\chi/2)]\right\}\frac{e^{-if\psi}}{\gamma}\Bigg\rangle_e \end{aligned} \tag{16}$$

where

$$K_f^{(m)}(\xi,\sigma) = (-1)^f \sum_{n=-\infty}^{\infty} J_n(f\xi)[(-1)^m J_{2n+f-m}(f\sigma) - J_{2n+f+m}(f\sigma)] \quad . \tag{17}$$

Including higher order source terms in the sum in Eq.(13) will not significantly improve the accuracy of the calculation since these terms are effectively averaged out by the electron ensemble, assuming the transverse density profile is smoothly varying.

A three-dimensional simulation code incorporating Eq.(13)-(17) has been written. A typical result of the code is the odd symmetry of the even harmonic radiation patterns as shown in Figure 4. Comparison of the simulation results with the power produced at the second through seventh harmonic of the Stanford Mark III FEL[13] were initially conducted. The simulation results were in good agreement with the experimental measurements for the first four harmonics as reported by Bamford and Deacon[14]. Closer comparisons of experiment and simulation will require more accurate measurement of the electron beam location in the wiggler and resolution of the transverse harmonic intensity profiles on a micropulse time scale.

The gradient of the transverse wiggler field also contributes to the radiation at the harmonic frequencies. However, this coupling is small for conventional FELs. The radiation into the even harmonics caused by gradients in the wiggler field will be $(\lambda_w/\pi r_e)^4$ times weaker than the radiation caused by gradients in the electron beam density[10]. This is what one would intuitively expect since the wiggler field gradient caused by the large separation of the wiggler magnets is much smaller than the density gradient inside the narrow electron beam.

Harmonic wiggler magnetic field components also affect the radiation at the harmonic frequencies[15]. Defining the amplitude of the harmonic wiggler vector potential at the l^{th} harmonic of the fundamental wiggler wavelength by $a_{w,l}$, the coupling coefficient, $bk_f^{(1)}(\xi,\sigma)$, in the monopole source term of Eq.(14) must be modified by the addition of the term

$$\begin{aligned} K = \sum_{l=3}^{\infty}\Bigg\{ & a_{w,l}\left(1+2\frac{lf\xi}{l^2-1}\right)\left[J_{\frac{f-l}{2}}(f\xi) - J_{\frac{l-f}{2}}(f\xi)\right] + \frac{f\xi a_{w,l}}{l-1}\left[J_{-\frac{f+(l-2)}{2}}(f\xi) - J_{-\frac{f-(l-2)}{2}}(f\xi)\right] \\ & + \frac{f\xi a_{w,l}}{l+1}\left[J_{-\frac{f+(l+2)}{2}}(f\xi) - J_{-\frac{f-(l+2)}{2}}(f\xi)\right]\Bigg\} \end{aligned} \tag{18}$$

where we assumed $a_{w,l} \ll a_{w,1}$. This term can either increase or decrease the coupling to the harmonics depending on the phase (sign) of the magnetic field $B_{w,l}$ in $a_{w,l}$. Harmonic wiggler vector potential components of 10% the fundamental value have been experimentally measured[16]. For conventional FEL configurations the harmonic wiggler components modify the harmonic radiated power by a factor of 2 or less.

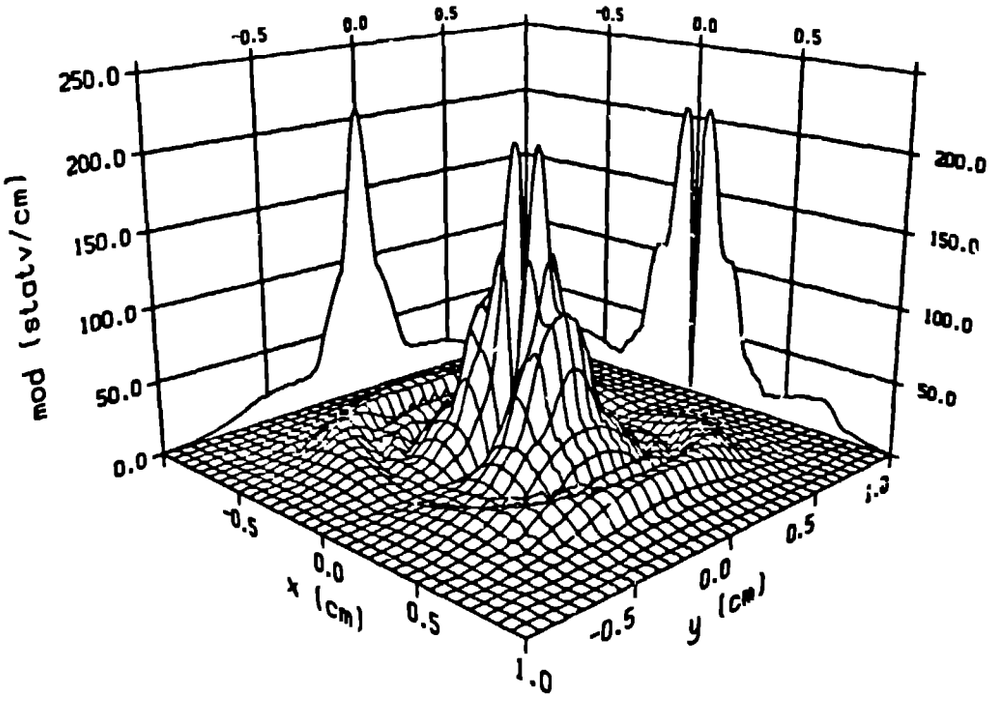

Figure 4. Plot of the magnitude of the electric field for the coherent-spontaneous emission at the second harmonic of a typical FEL amplifier. The negative amplitude lobe has been inverted for plotting purposes.

4. CONCLUSIONS

Formalisms now exist to calculate the spontaneous radiation of FELs at the harmonic frequencies in both the incoherent and coherent regimes. Simulations of harmonic emission for present FEL devices show good agreement with experimental measurements. Modeling of the harmonics in more complicated FEL configurations that include tapered wigglers, prebunchers and optical klystrons will be studied in the future. Multi-pass interactions including harmonic lasing[17,18] and interference effects of coherent-spontaneous emission[19] will also be examined.

5. ACKNOWLEDGMENT

The author wishes to thank C. Jim Elliott and Brian D. McVey for their continuing theoretical and computational collaboration. Work performed under the auspices of the U. S. Department of Energy and supported by the U. S. Army Strategic Defense Command.

6. REFERENCES

1. M. J. Schmitt and C. J. Elliott, "Even-harmonic generation in free-electron lasers", Phys. Rev. A 34 pp4843-4850, 1986.
2. Even harmonic radiation is also produced by misalignment of the electron beam and the wiggler axis. However, this radiation is of much lower intensity.
3. W. B. Colson, "The nonlinear wave equation for higher harmonics in free-electron lasers", IEEE J. Quantum Electron. QE-17 pp1417-1427 1981.
4. M. J. Schmitt, Harmonic Production in Free-Electron Lasers, Ph.D. Dissertation, UCLA 1987.
5. W. B. Colson, G. Dattoli and F. Ciocci, "Angular-gain spectrum of free-electron lasers", Phys. Rev. A 31 pp828-842 1985.
6. Kwang-Je Kim, 'An analysis of self-amplified spontaneous emission", Nucl. Instr. and Meth. A250

pp396-403 1986.
7. B. D. McVey, "Three-dimensional simulations of free-electron laser physics" Nucl. Instr. and Meth. **A250** pp449-455 1986.
8. M. J. Schmitt and C. J. Elliott, "Theory of harmonic radiation using a single-electron source model", Proceedings of the Eleventh International Conference on Free Electron Lasers, August 28 through September 1, 1989, held in Naples, FL, to be published.
9. J. D. Jackson, Classical Electrodynamics, p671, Wiley, New York, 1975.
10. M. J. Schmitt and C. J. Elliott, "Generalized derivation of free-electron laser harmonic radiation from plane-polarized wigglers", Phys. Rev. A, accepted for publication.
11. Pascal Elleaume, "Theory of the optical klystron", Nucl. Instr. and Meth. **A250** pp220-227 1986.
12. The paraxial wave equation invokes the slowly varying envelope approximation as discussed in: M. Sargent , M. O. Scully, and W. E. Lamb, Laser Physics, p100 Addison Wesley, Reading, 1974. The analogous expression for a Hermite-gaussian mode set is derived in reference [1].
13. S. V. Benson, et. al., "The Stanford Mark III infrared free electron laser", Nucl. Instr. and Meth. **A250** pp39-43 1986.
14. D. J. Bamford and D. A. G. Deacon, "Measurement of the coherent harmonic emission from a free-electron laser oscillator", Phys. Rev. Lett. **62** Number 10, pp1106-1109, 1989.
15. M. J. Schmitt and C. J. Elliott, "The effects of harmonic wiggler field components on free-electron laser operation", IEEE J. Quantum Electron. **QE-23** 1553-1557 1987.
16. K. Halbach, 'Permanent magnet undulators", Journal de Physique, Colloque C1, supplément au n°2 **Tome 44**, pp211-216, 1983.
17. S. V. Benson and J. M. J. Madey, "Demonstration of harmonic lasing in a free-electron laser", Phys. Rev. A **39** pp1579-1581 1989.
18. R. W. Warren, et. al., "Lasing on the third harmonic", Proceedings of the Eleventh International Conference on Free Electron Lasers, August 28 through September 1, 1989, held in Naples, FL, to be published.
19. B. A. Newnam, et. al., "Harmonic generation-strength and mode shape", Proceedings of the Eleventh International Conference on Free Electron Lasers, August 28 through September 1, 1989, held in Naples, FL, to be published.